

# Synthesis and Optical-Limiting Behavior of Hybrid Inorganic–Organic Materials from the Sol–Gel Processing of Organofullerenes

Michele Maggini,<sup>\*[b]</sup> Carla De Faveri,<sup>[b]</sup> Gianfranco Scorrano,<sup>[b]</sup> Maurizio Prato,<sup>\*[a]</sup> Giovanna Brusatin,<sup>[c]</sup> Massimo Guglielmi,<sup>\*[c]</sup> Moreno Meneghetti,<sup>[d]</sup> Raffaella Signorini,<sup>[d]</sup> and Renato Bozio<sup>\*[d]</sup>

**Abstract:** The optical-limiting properties of a series of novel [60]fullerene derivatives have been investigated in toluene solutions and in sol–gel glasses. Working at different wavelengths, it is found that the efficiency of the new compounds compares well with that of pristine C<sub>60</sub>. In particular, better performance of the organofullerenes is obtained when the pumping wavelength

approaches the triplet–triplet absorption maximum of the derivatives at ≈700 nm. The main component in the optical-limiting behavior is, in fact, ascribed to a reverse saturable absorption

**Keywords:** cycloadditions • fullerenes • molecular devices • nonlinear optics • sol–gel processes

mechanism. A relevant feature in the structure of the new organofullerenes is that a silicon-alkoxide moiety is covalently attached to C<sub>60</sub>. This guarantees the grafting of the fullerene spheroid to the silicon matrix during the sol–gel process. Some of the derivatives show remarkable solubility in THF, a solvent widely used in sol–gel processing, in which C<sub>60</sub> is itself insoluble.

## Introduction

The increasing spread of laser equipment and the prospective potential of laser-driven, all-optical devices have brought up the common problem of protecting optical sensors or the human eye from the damaging effects of high-energy laser light.<sup>[1]</sup> An attractive solution to this problem is represented by the optical limiters, that is, passive devices based on some kind of smart material that exhibits a high linear transmission at low energy inputs, but strongly and quickly reduces its transmittance when the intensity of the laser pulse approaches dangerous levels.<sup>[2]</sup>

For eye protection against laser pulses in the nanosecond range or shorter, the relevant physical quantity that an optical-limiting material should control is the fluence. The

phenomenon of reverse saturable absorption (RSA), exhibited by many classes of compounds, can provide the nonlinear response to the laser fluence that is required. RSA is active when an excited state that can be efficiently populated by optical pumping has an absorption cross-section ( $\sigma_E$ ) larger than that of the ground state ( $\sigma_G$ ) at the pumping wavelength. Metallophthalocyanines,<sup>[3]</sup> metal clusters,<sup>[4, 5]</sup> and fullerenes<sup>[6]</sup> are among the most efficient and most actively studied materials in this area.

Fullerene C<sub>60</sub><sup>[7, 8]</sup> can be considered a particularly promising material for optical-limiting purposes. It is well known that C<sub>60</sub> solutions show optical-limiting behavior that derives from a reverse saturable absorption mechanism, particularly for moderate input fluences.<sup>[6, 9–14]</sup> C<sub>60</sub>, in fact, exhibits a broad absorption spectrum, characterized by strong absorptions in the UV region and weaker absorptions extending over most of the visible region<sup>[15]</sup> where the first singlet excited state and the lowest energy triplet state show cross-sections larger than that of the ground state.<sup>[16]</sup> Since the efficient intersystem crossing from the singlet to the lowest triplet state ( $\phi_{ST} > 0.9$ ) occurs in about 1 ns,<sup>[15]</sup> the RSA observed on the picosecond time-scale is related to the singlet excited state,<sup>[11, 14]</sup> whereas that observed on the nanosecond time-scale relates to the lowest triplet state.<sup>[6, 14]</sup> At large input fluences (above some J cm<sup>-2</sup>) it has been shown that other limiting mechanisms, such as nonlinear scattering, become operative,<sup>[10, 17, 18]</sup> although RSA is always important.<sup>[18]</sup> This is particularly true for the solutions since it seems that such phenomena are less important for solid matrices containing C<sub>60</sub>.<sup>[19]</sup>

[a] Prof. M. Prato  
Dipartimento di Scienze Farmaceutiche  
Università di Trieste  
Piazzale Europa 1, I-34127 Trieste (Italy)  
Fax: (+39)04-052-572  
E-mail: prato@univ.trieste.it

[b] Dr. M. Maggini, Dr. C. De Faveri, Prof. G. Scorrano  
Centro Meccanismi di Reazioni Organiche del CNR  
Dipartimento di Chimica Organica  
Università di Padova (Italy)

[c] Prof. M. Guglielmi, Dr. G. Brusatin  
Dipartimento di Ingegneria Meccanica  
Università di Padova (Italy)

[d] Prof. R. Bozio, Dr. R. Signorini, Dr. M. Meneghetti  
Dipartimento di Chimica Fisica  
Università di Padova (Italy)

In their original paper, Tutt and Kost emphasized the fact that, in solution, the optical-limiting properties of  $C_{60}$  compare favorably with those of the existing materials currently under consideration for practical use.<sup>[6]</sup> Soon after, the same group reported the incorporation of  $C_{60}$  in poly(methyl methacrylate) (PMMA).<sup>[19]</sup> The results of their investigations led to the following conclusions: 1) the optical-limiting performance of the  $C_{60}$  samples appears promising with respect to other materials incorporated in PMMA; 2) the solid samples show a low damage threshold, which discourages the use of PMMA as a host material for practical applications.

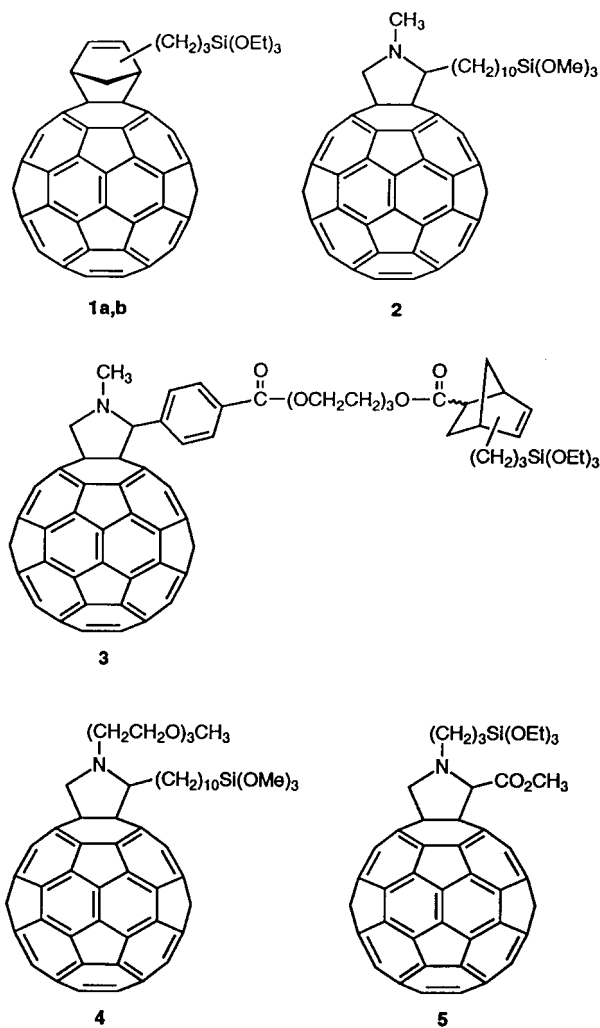
For practical uses as an optical limiter,  $C_{60}$  should be incorporated into materials that withstand high-energy laser pulses. Sol-gel glasses appear to be the materials of choice for these purposes. Glass, in fact, would easily survive the damaging action of lasers up to a reasonably high pulse energy. On the other hand, sol-gel processing allows the preparation of bulk glassy materials or thin films at low temperatures, under conditions compatible with most organic molecules.<sup>[20-25]</sup> The sol-gel process involves the polymerization of metal alkoxides. A solution (sol) is formed, which on standing, becomes a xerogel, and on heating densifies and turns into a glass or a ceramic material. In principle, any organic host molecule could be trapped in the inorganic matrix if it is present during the polymerization.

However,  $C_{60}$  is a difficult material to handle as it is sparingly soluble in aromatic hydrocarbons and not at all soluble in polar solvents.<sup>[26]</sup> Moreover,  $C_{60}$  has a high tendency to aggregate and to form clusters.<sup>[27]</sup> This results in non-homogeneous dispersions in the xerogel, and produces samples of low optical quality. Several attempts have been reported on methods to solve this problem by using a co-solvent for  $C_{60}$ <sup>[28, 29]</sup> or by diffusing  $C_{60}$  into the porous matrix.<sup>[30]</sup>

We have recently reported that higher quality and more concentrated glassy samples can be obtained by embedding in the sol-gel matrix  $C_{60}$  monoadducts instead of the pristine fullerene.<sup>[29]</sup> The photophysics of fullerene derivatives must still be fully explored, but the saturation of a double bond in

$C_{60}$  does not seem to affect significantly the photophysical properties of the derivatives with respect to  $C_{60}$ .<sup>[31]</sup> In fact, fullerene derivatives have a wider absorption range than  $C_{60}$ .<sup>[31]</sup> Moreover,  $C_{60}$  derivatives are usually more easily handled than  $C_{60}$  itself and, especially, their solubility in organic solvents can be modulated rather easily.

In this paper we report the design, synthesis, incorporation into sol-gel matrices, and optical-limiting properties, measured at different wavelengths in toluene solutions and in solid samples, of the derivatives **1-5** that exhibit the common feature of a silicon-alkoxide end-group covalently linked to the fullerene.<sup>[32, 33]</sup> The presence of the silicon-alkoxide group guarantees the chemical linking of the dopant to the oxide matrix,<sup>[20]</sup> which yields concentrated and homogeneous sols.



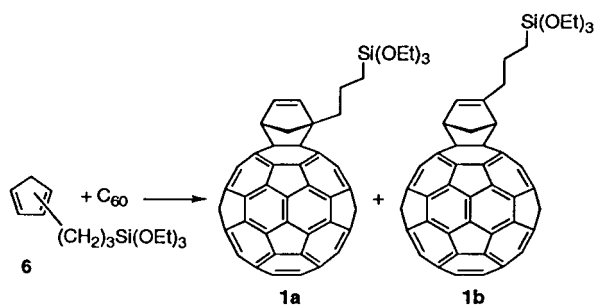
## Results and Discussion

**Synthesis of fullerene derivatives:** The chemical reactivity of fullerenes is now well established.<sup>[34, 35]</sup> The double bonds in  $C_{60}$  essentially behave as electron-deficient olefins and undergo addition reactions with a number of nucleophiles.<sup>[34]</sup> Electrophiles and radicals also add to  $C_{60}$ ,<sup>[36]</sup> but the best results, in terms of yields and characterization of the products, are obtained with cycloadditions.<sup>[34-36]</sup> Pioneering work by

**Abstract in Italian:** *Vengono riportate le proprietà di limitazione ottica di nuovi derivati fullerenici in soluzione e in matrici vetrose, preparate mediante la tecnica sol-gel. Misure a diverse lunghezze d'onda indicano che i nuovi composti hanno proprietà superiori a quelle del fullerene non modificato quando la lunghezza d'onda della luce laser incidente è prossima al massimo di assorbimento dello stato eccitato di tripletto, a circa 700 nm. L'effetto di limitazione ottica è attribuito al meccanismo di assorbimento saturabile inverso. Una caratteristica strutturale importante dei nuovi derivati consiste nella presenza di un gruppo trialcossilile legato covalentemente alla sfera fullerenica. Questo permette un attacco covalente alla matrice silicea durante il processo sol-gel. Inoltre, alcuni derivati possiedono un'elevata solubilità in tetraidrofurano, il solvente usato nel processo sol-gel, nel quale il  $C_{60}$  non modificato non è solubile.*

Wudl and co-workers<sup>[37, 38]</sup> showed that 1,3-dipoles are particularly well suited for reactions with  $C_{60}$ , but it was later shown by several other groups<sup>[39–42]</sup> that 1,3-dienes (such as cyclopentadiene)<sup>[43, 44]</sup> also react very well. The cycloaddition is reversible,<sup>[45]</sup> but the addition product can be isolated and characterized.

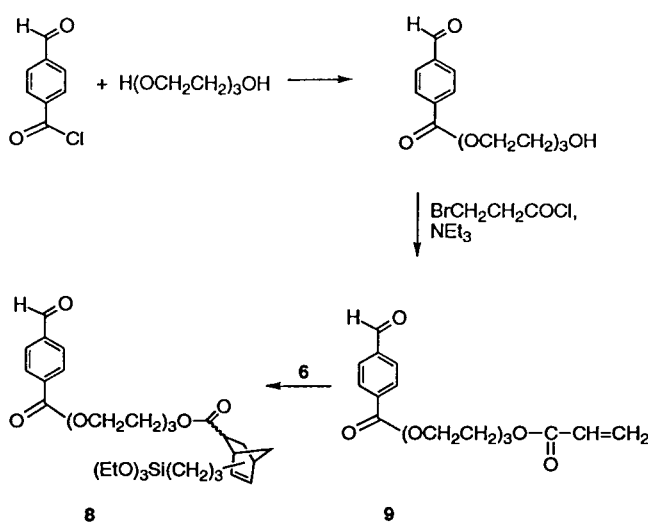
A very quick route to silicon-alkoxide-functionalized  $C_{60}$  is provided by the reaction of cyclopentadiene **6** (obtained by thermal cycloreversion of the commercially available dimer), see Scheme 1. The reaction was carried out in toluene at room



Scheme 1.

temperature and the monoaddition product was isolated in 53% yield (along with 25% of recovered  $C_{60}$ ). Due to the facile [1,5]-hydrogen shift in cyclopentadienes, both the starting cyclopentadiene and the cycloadduct were formed in a mixture of two isomers. This could be easily seen from the  $^1H$  NMR spectrum, where a ratio of about 1:1 for **1a/1b** was observed. Analysis of the mixture by HPLC (polystyrene gel, toluene) gave a single peak and elemental analysis showed the mixture to be pure. The isomeric mixture was considered suitable for the purposes of the present work. In fact, it was not expected that the position of the side chain in the bicycloheptene ring would influence significantly the photophysics of the fullerene moiety.

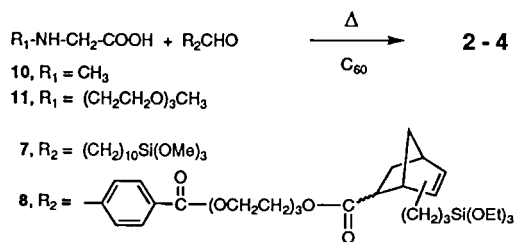
However, for efficient control of the structure and of the solubility of the material, a more versatile approach was desirable. For this purpose, the addition of azomethine ylides to  $C_{60}$  was employed. The condensation of an  $\alpha$ -amino acid with an aldehyde produces the reactive 1,3-dipole which then adds irreversibly to  $C_{60}$  to give  $C_{60}$ -fused pyrrolidines (fulleropyrrolidines).<sup>[46–48]</sup> In principle, the silicon-alkoxide functionality, needed for grafting the fullerene derivative on to the silica network, can be located either on the amino acid or on the aldehyde, or even on both partners. For a reasonably easy experimental route, we decided to make the aldehyde bear the alkoxy silane group. Thus, aldehyde **7**,  $(CH_3O)_3Si(CH_2)_{10}CHO$ , was obtained by hydrosilylation of 10-undecenal with trimethoxysilane in the presence of catalytic hexachloroplatinic acid.<sup>[49]</sup> The somewhat more complex aldehyde **8**, whose triethylene glycol (TEG) chain should readily improve the solubility of the fullerene derivative, was prepared from TEG and 4-formyl benzoyl chloride, followed by reaction of the resulting ester-alcohol with 3-bromopropionyl chloride in excess triethylamine (Scheme 2). The aldehyde-TEG-functionalized acrylate **9** thus obtained was allowed to react with cyclopentadiene **6** in 1,2-dichlorobenzene at 180 °C, yielding **8**



Scheme 2.

as an analytically pure (from elemental analysis) mixture of stereoisomers.

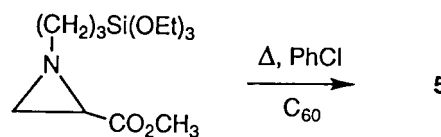
Both aldehydes **7** and **8** reacted readily with *N*-methyl glycine (sarcosine) **10** and  $C_{60}$  to form the substituted pyrrolidines **2** and **3** in 32–33% yield, along with 40–50% of recovered  $C_{60}$  (Scheme 3).



Scheme 3.

To improve further the solubility of the fullerene derivatives, *N*-substituted glycine **11**<sup>[50, 51]</sup> was condensed with aldehyde **7** in the presence of  $C_{60}$ , which afforded fulleropyrrolidine **4** (Scheme 3).

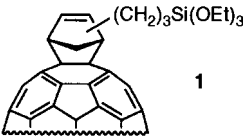
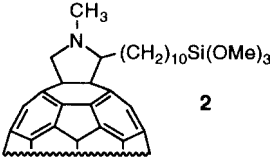
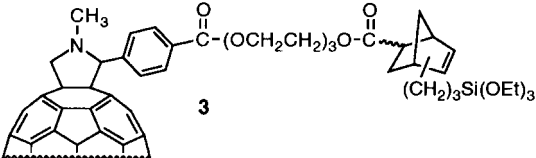
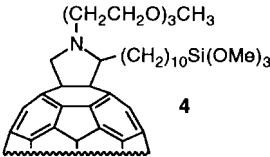
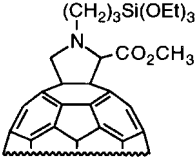
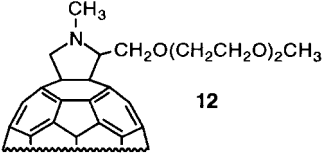
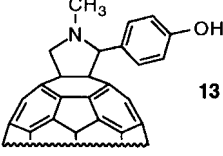
Alternatively, the thermal ring-opening of aziridines with electron-attracting substituents in the presence of  $C_{60}$  also generated fulleropyrrolidines (Scheme 4).<sup>[47]</sup>



Scheme 4.

The sol–gel process can be performed preferentially in ethanol or THF. The latter solvent is much better for dissolving fullerene derivatives, and so the solubility of derivatives **1–5** was then checked in THF. The results are reported in Table 1, along with the solubility of two compounds, **12** and **13**, that do not contain a silicon-alkoxide moiety, but were used previously for optical-limiting (OL)

Table 1. Solubilities in THF of fullerene derivatives **1–5** and **12** and **13**.

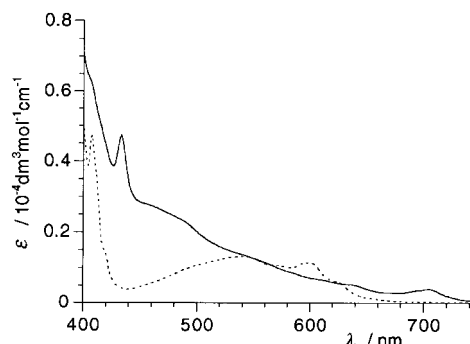
Compound	mg mL <sup>-1</sup>
	27
	27
	61
	216
	43
	31
	1.0

purposes.<sup>[29]</sup> The solubility of compounds **1–5** and **12**, **13** in THF was measured by preparation of a saturated solution with centrifugation for 5 min at 14000 rpm to separate the solid completely and to obtain clear solutions. The concentrated solutions were then diluted and their absorbances determined from a calibration line.

From inspection of Table 1, it is possible to compare the contribution of the many moieties with the solubility of the compounds studied. From our sol–gel benchmark compound **12**,<sup>[29]</sup> the solubility can be improved by two orders of magnitude, such as with **4**, where the solubilizing efficiency of the trioxadecane chain is synergistically combined with the long hydrocarbon chain that bears the silicon-alkoxide group.

### Optical-limiting properties of compounds **1–5** in toluene.<sup>[32]</sup>

The linear optical properties of fulleropyrrolidines are illustrated in Figure 1, where the representative visible and near-infrared absorption spectrum for compound **2** is shown

Figure 1. UV/Vis spectra of solutions of **2** (—) and C<sub>60</sub> (---) in toluene.

and compared with that of C<sub>60</sub>. The spectra of the derivatives are quite similar to those of other 1,2-dihydrofullerenes<sup>[31, 52–54]</sup> and bear a general resemblance to that of C<sub>60</sub>.<sup>[15, 55]</sup> There are, however, some differences which may significantly affect the RSA properties. In particular, after a typical narrow peak around 430 nm, the absorption of **1–5** decreases slowly in the visible region and extends through longer wavelengths in the near-infrared region (with a weak band around 700 nm), where C<sub>60</sub> does not absorb. This behavior favors broader reverse saturable absorption (RSA) activity of the derivatives, since it lowers the saturation value of the fluence (vide infra), which makes it possible to exploit the RSA mechanism fully.<sup>[56, 57]</sup>

Other photophysical properties of the derivatives important to the RSA behavior are also similar to those of C<sub>60</sub>. It is, in fact, known that the intersystem crossing is almost unitary and that the triplet absorption spectrum has an intense band in the near-infrared with a maximum at about 700 nm.<sup>[31, 52–54]</sup> Different values have been measured for the peak absorption cross-section of the triplet spectrum ( $\sigma_T$ ) of different 1,2-dihydrofullerenes. It is commonly reported that the absorption maximum has a lower value<sup>[31, 52–54]</sup> than that of C<sub>60</sub> at 750 nm,<sup>[16]</sup> but for one fulleropyrrolidine derivative it was found to be larger.<sup>[53]</sup> In all cases, the maximum of the triplet spectrum is shifted with respect to that of C<sub>60</sub>. This means that, on approaching the near-infrared region, a strong RSA should be observed at shorter wavelength than for C<sub>60</sub>.

In the present work, the OL properties of the fullerene derivatives have been investigated by measuring the fluence dependence of the transmission of their solutions in toluene with different laser wavelengths for comparison with those of C<sub>60</sub>. Figure 2 depicts the measured nonlinear transmittances for **1** in toluene and its comparison with C<sub>60</sub> at 532 and 652 nm.

It should be noted that the reported fluences are nominal values obtained simply by dividing the incident pulse energy by the cross-sectional area at the beam waist. Therefore, the input fluence represents the maximum value that would be obtained if no absorption of the incident beam by the sample occurred. The measured linear absorbances ( $A_0$ ) and the ratio

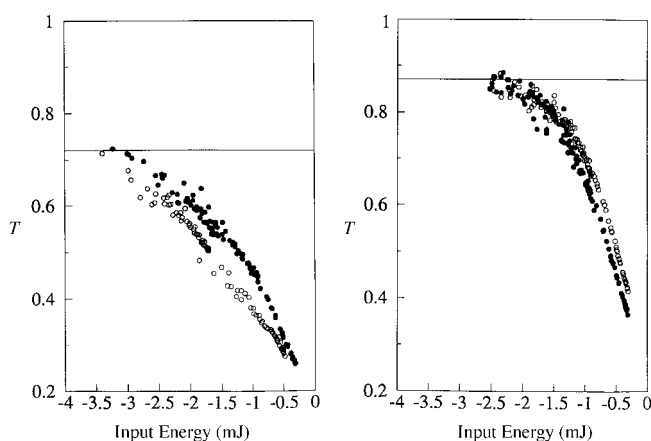


Figure 2. Nonlinear transmittance  $T$  versus incident fluence at a) 532 nm and b) 652 nm for **1** (■) and for  $C_{60}$  (○) in toluene. The linear transmittance was 72 % at 532 nm and 87 % at 652 nm for solutions of both compounds.

of the nonlinear absorbances at  $20 \text{ J cm}^{-2}$  to the linear ones ( $A_{20}/A_0$ ) are reported in Table 2 for all the compounds.

Table 2. Experimental linear ( $A_0$ ) and relative nonlinear absorbances at  $20 \text{ J cm}^{-2}$  ( $A_{20}/A_0$ ) for  $C_{60}$  and for the fullerene derivatives in toluene.

	532	[nm]	652	[nm]
	$A_0$	$A_{20}/A_0$	$A_0$	$A_{20}/A_0$
$C_{60}$	0.143	4.2	0.063	5.0
$C_{60}$	0.265	2.5		
<b>1</b>	0.143	3.7	0.060	6.8
<b>2</b>	0.225	3.1	0.083	5.6
<b>3</b>	0.301	2.2	0.064	4.5
<b>4</b>	0.183	3.4		
<b>5</b>	0.147	4.3		
<b>12</b>	0.155	3.5	0.063	5.3

From Figure 2 and Table 2 it is possible to see that solutions of the derivatives give better performance, with respect to  $C_{60}$ , in the red spectral region at 652 nm, whereas the contrary is true at 532 nm. This is consistent with an RSA mechanism, considering the photophysical properties of the triplet states of the derivatives which show an absorption maximum at 700 nm instead of at 750 nm as exhibited by  $C_{60}$ .

It can be easily shown that, with nanosecond pulses and with the photophysical properties of the fullerenes, one can approximately describe the RSA phenomenon by focusing on only the ground state and the lowest triplet state, and by neglecting the population of all the other electronic or vibronic states. Under these circumstances, one can define a fluence-dependent effective absorption cross-section  $\sigma_{\text{eff}}$  [Eq. (1)] which contains, as a parameter, the saturation

$$\sigma_{\text{eff}} = \sigma_T + (\sigma_G - \sigma_T) \exp(-F/F_S) \quad (1)$$

fluence  $F_S = hc/(\Phi_{ST}\sigma_G\lambda)$ . The value of  $F \equiv F(z)$  to be inserted in the equation for  $\sigma_{\text{eff}}$  is a function of the position  $z$  along the beam path that should take into account the absorption processes occurring during the propagation. For thick samples, this would imply integration of appropriate differential equations.<sup>[11]</sup> However, to capture the essential ingredients of the phenomenon, one can use the expression for thin films

with an effective value for the sample thickness. For fluence values  $F_0$  exceeding  $F_S$  we get Equation (2) where  $N_0$  is the

$$\sigma_{\text{eff}}(F_0) \approx \sigma_T + (\sigma_G - \sigma_T) \exp \left[ -\frac{F_0 \exp(-N_0 \sigma_T d_{\text{eff}}) \Phi_{ST} \sigma_G \lambda}{hc} \right] \quad (2)$$

number density of fullerene molecules, and  $d_{\text{eff}}$  the effective sample thickness. The curves in Figure 3 exemplify the dependence on the sample concentration of the ratio  $\sigma_{\text{eff}}(20)/\sigma_{\text{eff}}(0) = \sigma_{\text{eff}}(20)/\sigma_G$ , where  $\sigma_{\text{eff}}(20)$  is the value of the absorption cross-section at an input fluence of  $20 \text{ J cm}^{-2}$ . Figure 3 also shows the wavelength dependence of the saturation fluence.

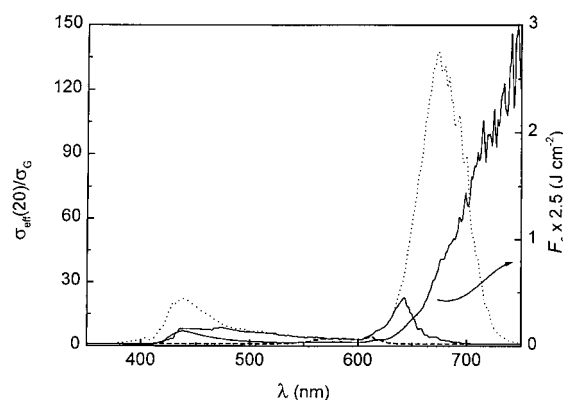


Figure 3. Calculated ratio of the effective absorption cross-section ( $\sigma_{\text{eff}}$ ) at  $20 \text{ J cm}^{-2}$  to that of the ground state ( $\sigma_G$ ) (see text) as a function of wavelength for different sample concentrations:  $1 \times 10^{-2} \text{ mol dm}^{-3}$  (---),  $5 \times 10^{-3} \text{ mol dm}^{-3}$  (—),  $4 \times 10^{-3} \text{ mol dm}^{-3}$  (····). The saturation fluence ( $F_S$ ) multiplied by 2.5 as a function of wavelength is also reported.

The values of  $\sigma_G$  and  $\sigma_T$  and their wavelength dependence are those for  $C_{60}$  taken from the literature.<sup>[16]</sup> Note that  $\sigma_{\text{eff}}$  quickly drops in the red before reaching the peak wavelength of the triplet absorption spectrum ( $\approx 750 \text{ nm}$ ). This results from the fact that  $\sigma_G$  practically vanishes for  $\lambda > 700 \text{ nm}$ , making the saturation fluence prohibitively large. The peak value of  $\sigma_{\text{eff}}(20)/\sigma_G$  is also a function of the thickness and/or the concentration, and it may be considerably lower than  $\sigma_T/\sigma_G$ .

From the foregoing discussion, the measured ratio  $A_{20}/A_0$  should approach  $\sigma_T/\sigma_G$  if the OL properties are due to RSA and if the laser fluence is much greater than the saturation fluence  $F_S$  at all points along the beam path inside the sample. A number of factors may be responsible for a value of  $A_{20}/A_0$  that is below or even above  $\sigma_T/\sigma_G$ . As the concentration increases, larger and larger values of the incoming pulse energy are required to keep  $F(z) \gg F_S$  at each point  $z$  in the sample, and eventually the transfer of population to the triplet state becomes incomplete and  $A_{20}/A_0$  gets smaller than  $\sigma_T/\sigma_G$ . As already mentioned, nonlinear scattering may lead to an apparent enhancement of the OL efficiency if the acceptance angle of the detector is small and most of the scattered light does not contribute to the measured signal. We have compared a typical nonlinear transmission curve measured for  $C_{60}$  in toluene with a curve calculated by integration of the appropriate master equations based on the RSA model with account of the beam propagation properties used in our

experiment.<sup>[55, 56]</sup> It turns out that at  $20 \text{ J cm}^{-2}$  nonlinear scattering, or any other OL mechanism, contributes almost 30% of the measured decrease in transmittance. Of course, this implies that  $A_{20}/A_0$  appears to be greater than  $\sigma_T/\sigma_G$ . The data in Table 2 suggest that both effects are present in our measurements and that their balance depends on the linear transmittance, that is, the concentration of the samples in solution. In fact, it can be seen that the measured  $A_{20}/A_0$  ratio at 532 nm is 4.2 and 2.5 for  $C_{60}$  solutions with a linear transmittance of 72 and 54%, respectively. By comparison, the estimated  $\sigma_T/\sigma_G$  ratio is in the range 2.7–3.2.

The important conclusions that can be drawn from the data of Table 2 are: (1) by comparison with the optical-limiting properties of  $C_{60}$ , the behavior of the fullerene derivatives presented in this paper is very similar, with an enhanced efficiency in the red spectral region; (2) in all cases the RSA mechanism appears to dominate the OL process.<sup>[13, 32]</sup>

### Incorporation of the fullerene derivatives 1–5 in sol–gel glasses:

Silica sols were prepared from tetraethoxysilane (TEOS) and methyltriethoxysilane (MTES) as silica precursors. Monoliths were obtained with a sol modified by partial or total substitution of TEOS with MTES. A solution with molar ratios for TEOS/MTES of 2:3 and for (TEOS + MTES)/ $H_2O/HCl/EtOH$  of 1:3.4:0.006:1 was prehydrolyzed for 4 h and then mixed with the appropriate derivative dissolved in THF. Sonication was applied to achieve suitable dispersion of the fullerenes in the solvent and in the sol–gel solutions. The final dilution of the sol, measured by  $SiO_2$  concentration, was never less than  $60 \text{ g L}^{-1}$  for the most concentrated solutions of the fullerene derivatives. The maximum concentration of a  $C_{60}$  derivative obtained in homogeneous solutions was about  $8 \times 10^{-3} C_{60}/SiO_2$  in the case of compound **5**.

Films were deposited from these sols by spinning at 2000 rpm and were dried at  $60^\circ\text{C}$ . Monolithic xerogels were also produced by leaving the sol in a closed vessel at  $60^\circ\text{C}$ . Gelation took place in about 3 days. Transparent bulk samples in the form of disks of 15 mm diameter and 3 mm thickness were produced. The density of the bulk samples, measured in ethanol with a picnometer, was  $1.412 \text{ g cm}^{-3}$  and the fullerene concentration was  $1.66 \times 10^{-3} \text{ mol l}^{-1}$ .

The films and bulks are environmentally stable, and even after several months, materials exposed to air and light did not show any change in their optical properties (linear and nonlinear).

### Optical limiting of the fullerene derivatives embedded in sol–gel matrices:

Optical-limiting measurements of solid samples containing  $C_{60}$  or other fullerene derivatives have been reported.<sup>[19, 29, 58–62]</sup> Usually  $C_{60}$  can be included only at low concentration and the possible clustering of the molecules causes optical inhomogeneity in the sample. In one case, in order to overcome these problems,  $C_{60}$  was functionalized with silicon-alkoxide groups.<sup>[60]</sup> However, the functionalization was achieved in an uncontrolled manner, such that the  $C_{60}$  derivatives included in the matrix were mixtures of multiple adducts that were not characterized further.

The linear optical spectrum of **2** and **3** embedded in a bulk sample is shown in Figure 4. Some features of the linear spectrum of the solution (see Figure 1) appear to be smoother, probably due to interactions of the molecules with the

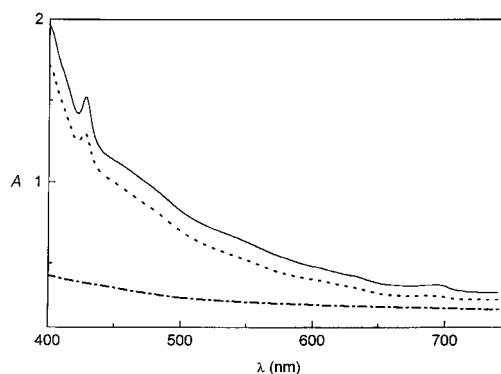


Figure 4. UV/Vis spectra of **2** (---) and **3** (—) in a sol–gel matrix;  $A$  = absorbance in arbitrary units.

disordered sol–gel matrix, which causes inhomogeneous broadening. However, to our knowledge, this represents the first example where solid thin films of  $C_{60}$  derivatives show fine structure in the visible region with typical peaks at  $\approx 430$  and  $700 \text{ nm}$ , which might be taken as evidence of lack of clustering.

Attempts to observe optical-limiting behavior for films obtained by spinning gave inconclusive results due to the low optical density that was attainable for a single thin film. We have thus measured the optical-limiting properties of sol–gel monolithic slabs that incorporate the fullerene derivatives **1–5** and  $C_{60}$ . The fluence-dependent nonlinear transmittance at  $652 \text{ nm}$  of the sample containing **2** is reported in Figure 5 as a typical example.

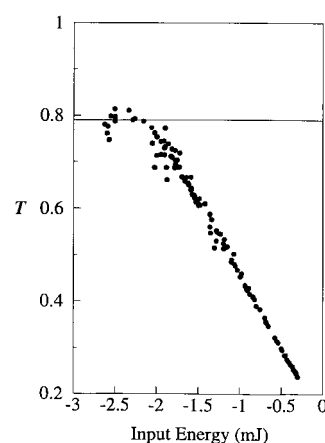


Figure 5. Nonlinear transmittance versus incident fluence at  $652 \text{ nm}$  of a sol–gel slab of  $0.25 \text{ cm}$  thickness containing compound **2** with a molar ratio  $2:SiO_2$  of  $1 \times 10^{-4}$ .  $T$  = transmittance.

The low threshold for the nonlinear behavior observed for the solutions (see Figure 2b) is retained in the sol–gel material. Furthermore, the damage threshold was not reached before  $30 \text{ J cm}^{-2}$ . This is a very important feature of the sol–gel matrix since, as previously noted, a polymer-like PMMA

used as a solid host matrix could only withstand less than  $2 \text{ J cm}^{-2}$ .<sup>[19]</sup> In Table 3 we report a summary of the OL data that were obtained for our bulk samples.

Table 3. Experimental linear ( $A_0$ ) and relative nonlinear absorbances at  $20 \text{ J cm}^{-2}$  ( $A_{20}/A_0$ ) for fullerene derivatives embedded in sol–gel slabs<sup>[a]</sup> of thickness  $d$ .

	$d$ [cm]	532 $A_0$	[nm] $A_{20}/A_0$	652 $A_0$	[nm] $A_{20}/A_0$
1	0.15	0.155	2.3	0.187	1.6
2	0.25	0.522	2.0	0.102	5.4
3	0.20	0.347	1.9	0.276	2.5
12 <sup>[b]</sup>	0.23	0.420	1.5	0.259	2.2

[a] Fullerene derivatives to silica molar ratio is  $1.0 \times 10^{-4}$ . The estimated conversion factor to obtain  $\text{mol dm}^{-3}$  is about 9–10. [b] Molar ratio  $\mathbf{1a}/\text{SiO}_2 = 5.4 \times 10^{-5}$ .

As in the case of the solutions, the optical-limiting behavior is larger at 652 than at 532 nm. In general, however, the values of the absorption ratio ( $A_{20}/A_0$ ) are lower than those measured for the solutions. This can be partly understood by considering that, as previously observed,<sup>[19]</sup> for solid samples the nonlinear scattering seems to contribute to the response much less than for solutions. However, taken alone, this cannot explain the large differences in the measured values of  $A_{20}/A_0$ , nor the fact that in the case of derivative **2** the value measured at 652 nm was very close to that of the solution. Measurements taken from different spots in the same sample sometimes gave different results. Larger  $A_{20}/A_0$  values were always obtained for the spots that gave higher linear transmittance. Note, in fact, that the linear absorbances reported in Table 3 are larger than are expected on the basis of Beer's law, assuming that the extinction coefficient of the fullerenes in sol–gel glasses does not differ markedly from that of the solutions. This suggests that some linear scattering is still present in our samples, despite the fact that the covalent linking of the fullerene derivatives to the silica matrix by their silicon-alkoxide functionality should prevent the formation of clusters. The likely origin of the linear scattering observed for thick sol–gel slabs is the presence of structural inhomogeneities that form during densification and that can hardly be controlled with the sol–gel procedures employed in this work. The decreased OL efficiency of the sol–gel slabs is then ascribed to the reduced apparent transmittance (increased  $A_0$ ) measured by our limited aperture detection, as well as to the effect of the linear scattering on the intensity distribution and waist of the laser beam, and hence on the actual value of the laser fluence. However, we note that the nonlinear induced optical density ( $A_{20} - A_0$ ) of the solid samples at  $20 \text{ J cm}^{-2}$  is of the order of 0.4, a figure similar to that observed for the solutions.

## Conclusion

Important advances towards the goal of using fullerenes for the preparation of smart materials with OL properties of practical relevance have been made. The low solubility of  $\text{C}_{60}$  in polar solvents and its tendency to form clusters in a polar

environment have been overcome by suitable functionalization both with solubilizing chains and with silicon-alkoxide groups. The latter groups enable the fullerenes to link covalently to the silica matrix. Environmentally stable sol–gel glasses containing a high concentration of  $\text{C}_{60}$  derivatives have been prepared as both thin films (obtained by spinning on glass substrates) and thick monolithic slabs.

The optical-limiting properties of the new fullerene derivatives in toluene at various visible wavelengths are comparable with the corresponding properties of  $\text{C}_{60}$ . The derivatives offer somewhat better performances in the red, as can be expected from the shift to shorter wavelengths of the triplet absorption peak. However, the actual relative absorbance at high fluence ( $A_{20}/A_0$ ) depends on several factors such as the ground and triplet state absorption cross-sections at the given wavelength, the sample concentration, and the fluence profile  $F(z)$ .

With regard to the sol–gel glasses, the important result is that the new derivatives provide access to materials with a wide range of concentrations of fullerenes covalently linked to the silica matrix. The presence of residual linear scattering (likely to be due to structural inhomogeneities) affects the measurements of the OL properties on thick slabs. Nonetheless, the induced absorbance ( $A_{20} - A_0$ ) is, in most cases, similar to that obtained for solution samples, and the threshold for laser damage is very high compared, for example, with polymer matrices. We are currently working to improve the optical quality of the sol–gel materials. In principle, it should be possible to obtain sizeable OL behavior from films prepared by spinning, provided their thickness can be increased to the tens-of-microns range. This would open the way to the preparation of multilayer structures that allow optimization of the OL properties through the full exploitation of the RSA mechanism in fullerenes.<sup>[56, 57]</sup>

## Experimental Section

Details regarding instrumentation used to characterize the compounds considered in this paper have been described elsewhere.<sup>[48]</sup> Silica films were deposited by spinning (2000 rpm) with an EMHART Dynapert apparatus. Film thickness was measured with an Alpha Step 200 Tencor profilometer.

**Materials:**  $\text{C}_{60}$  was purchased from Bucky USA (99.5%). (3-Cyclopentadienyl)propyltriethoxysilane dimer, 3-aminopropyltriethoxysilane, and trimethoxysilane were purchased from ABCR-Germany. All other reagents were used as bought from Aldrich. Tetrahydrofuran, employed for UV/Vis measurements and sol–gel film preparation, was distilled prior to use. *N*-(3,6,9-Trioxadecyl)glycine (**11**),<sup>[51]</sup> *N*-[3-(triethoxysilyl)propyl]-2-carbomethoxy-3,4-fulleropyrrolidine (**5**),<sup>[50]</sup> *N*-methyl-2-(3,6,9-trioxadecyl)-3,4-fulleropyrrolidine (**12**),<sup>[29]</sup> and *N*-methyl-2-(4-hydroxyphenyl)-3,4-fulleropyrrolidine<sup>[29]</sup> (**13**) were prepared as previously described.

**Addition of (3-cyclopentadienyl)propyltriethoxysilane to  $\text{C}_{60}$ : synthesis of derivative **1**:** A solution of  $\text{C}_{60}$  (50 mg, 0.069 mmol) and the cyclopentadienyl monomer **6** (20 mg, 0.074 mmol) was stirred at ambient temperature for 3.5 h, after which the solvent was removed in vacuo. The residue was purified by flash chromatography ( $\text{SiO}_2$ , eluent: toluene,  $R_f = 0.5$ ) to afford **1** (36 mg, 53%) as a mixture of isomers (**1a**, **b**, see text) along with unreacted  $\text{C}_{60}$  (12.5 mg, 25%).  $^1\text{H NMR}$  (250 MHz,  $\text{C}_6\text{D}_6$ ):  $\delta = 0.70$ – $0.80$  (m, 4H), 1.18 (t,  $J = 6.94$  Hz, 9H), 1.18 (t,  $J = 6.94$  Hz, 9H), 1.80–1.99 (m, 4H), 2.38–2.41 (m, 1H), 2.67–2.69 (m, 1H), 2.42 (d,  $J = 9.50$  Hz, 1H), 2.43 (d,  $J = 9.14$  Hz, 1H), 2.59 (td,  $J = 1.46$  Hz,  $J = 7.68$  Hz, 2H), 3.06 (d,  $J = 9.50$  Hz, 1H), 3.36 (d,  $J = 9.14$  Hz, 1H), 3.76 (q,  $J = 6.94$  Hz, 6H), 3.77 (q,  $J = 6.94$  Hz, 6H), 4.17 (m, 1H), 4.27 (m, 1H), 4.32 (m, 1H), 6.48 (s, 1H),

6.75 (d,  $J = 5.48$  Hz, 1H), 6.87 (m, 1H);  $^{13}\text{C}$  NMR (62.9 MHz,  $\text{CD}_2\text{Cl}_2$ ):  $\delta = 19.98, 20.90, 27.70, 27.76, 29.99, 30.26, 43.82, 45.03, 54.47, 56.57, 65.49, 66.16, 67.34, 69.51, 75.05, 84.54, 85.14, 86.35, 87.94, 139.11, 146.03, 146.11, 146.20, 146.35, 146.47, 146.56, 146.69, 146.82, 148.52, 148.58, 148.78, 148.81, 148.87, 149.04, 149.81, 150.77, 150.89, 151.05, 151.10, 151.32, 151.53, 151.58, 151.65, 151.77, 152.07, 153.34, 153.42, 153.48, 153.62, 154.21, 154.26, 154.31, 154.36, 154.46, 154.85, 154.93, 155.01, 155.13, 155.20, 155.24, 155.34, 155.50, 155.64, 156.08, 156.33, 162.19, 163.97, 164.32, 164.73, 164.80, 165.71, 165.75, 166.48, 166.95; IR (KBr):  $\tilde{\nu} = 2968, 2922, 2879, 1165, 1102, 1078, 957, 794, 527$   $\text{cm}^{-1}$ ; MALDI-MS (MW = 990):  $m/z$ : 828 [ $M - \text{Si}(\text{OEt})_3 + \text{H}$ ] $^+$ , 720 [ $\text{C}_{60}$ ] $^+$ ; UV/Vis (THF):  $\lambda_{\text{max}}$  ( $\epsilon$ ) = 256 (94600), 322 (30500), 432 (3300), 632 (400);  $\text{C}_{72}\text{H}_{20}\text{O}_3\text{Si}$ : calcd C 89.68, H 2.64; found C 89.32, H 2.39.$

**General procedure for the synthesis of fulleropyrrolidines 2–4:** A solution of  $\text{C}_{60}$ , the appropriate aldehyde, and *N*-substituted glycine in toluene was refluxed and the solvent was then removed under reduced pressure. The product was purified by flash chromatography ( $\text{SiO}_2$ ) with toluene to remove the unreacted  $\text{C}_{60}$ , and then with mixtures of toluene/ethyl acetate. The compounds were dissolved in the minimum amount of toluene and precipitated by addition of acetonitrile.

***N*-Methyl-2-(10-decyltrimethoxysilyl)-3,4-fulleropyrrolidine (2):** Starting materials:  $\text{C}_{60}$  (59.7 mg, 0.083 mmol), *N*-methylglycine (17.3 mg, 0.19 mmol), 11-trimethoxysilyl undecanal **7** (24.1 mg, 0.083 mmol) dissolved in toluene (55 mL) (5 h). Eluent: toluene, then toluene/ethyl acetate 9:1,  $R_f = 0.5$ ; yield = 27 mg (31%) along with unreacted  $\text{C}_{60}$  (29 mg, 48%).  $^1\text{H}$  NMR (250 MHz,  $\text{C}_6\text{D}_6$ ):  $\delta = 0.76\text{--}0.82$  (m, 2H), 1.33–1.41 (m, 12H), 1.61–1.67 (m, 2H), 1.90–1.94 (m, 2H), 2.36–2.60 (m, 2H), 2.67 (s, 3H), 3.51 (s, 9H), 3.76 (t,  $J = 5.55$  Hz, 1H), 3.80 (d,  $J = 9.82$  Hz, 1H), 4.40 (d,  $J = 9.82$  Hz, 1H);  $^{13}\text{C}$  NMR (62.9 MHz,  $\text{C}_6\text{D}_6$ ):  $\delta = 9.93, 23.28, 27.60, 29.80, 29.84, 29.93, 29.97, 30.60, 31.27, 33.53, 39.50, 50.30, 70.23, 70.65, 76.80, 78.26, 135.87, 136.25, 136.68, 137.63, 139.99, 140.17, 140.53, 140.59, 142.02, 142.06, 142.19, 142.42, 142.48, 142.56, 142.98, 143.05, 143.45, 143.56, 144.71, 144.77, 144.93, 145.11, 145.53, 145.58, 146.66, 145.75, 145.80, 145.90, 146.13, 146.26, 146.36, 146.40, 146.51, 146.60, 146.71, 146.90, 147.15, 147.48, 147.52, 154.20, 154.94, 155.02, 157.14; IR (KBr):  $\tilde{\nu} = 2921, 2849, 2776, 1462, 1086, 805, 527$   $\text{cm}^{-1}$ ; MALDI-MS (MW = 1037):  $m/z$ : 1036 [ $M - \text{H}$ ] $^+$ ; UV/Vis (THF):  $\lambda_{\text{max}}$  ( $\epsilon$ ) = 254 (104800), 308 (34400), 431 (3800), 630 (340);  $\text{C}_{70}\text{H}_{35}\text{NO}_3\text{Si}$ : calcd C 87.92, H 3.40, N 1.35; found C 87.60, H 3.30, N 1.45.$

**Fulleropyrrolidine 3:** Starting materials:  $\text{C}_{60}$  (43 mg, 0.060 mmol), *N*-methylglycine (10.8 mg, 0.12 mmol), aldehyde **8** (36.3 mg, 0.060 mmol) dissolved in toluene (40 mL, 3.5 h). Eluent: toluene/ethyl acetate, gradient from 9:1 to 7:3,  $R_f = 0.4\text{--}0.5$ ; yield = 26.6 mg (33%) along with unreacted  $\text{C}_{60}$  (16 mg, 37%).  $^1\text{H}$  NMR (250 MHz,  $\text{CS}_2/\text{C}_6\text{D}_6$  2:1):  $\delta = 0.53\text{--}0.67$  (m), 0.90–1.10 (m), 1.17 (t,  $J = 6.94$  Hz), 1.27–1.39 (m), 1.42–1.60 (m), 1.68–1.77 (m), 1.78–2.15 (m), 2.59 (s), 2.60–3.07 (m), 3.38–3.45 (m), 3.46–3.55 (m), 3.75 (q,  $J = 6.94$  Hz), 3.80–4.06 (m), 4.03 (d,  $J = 9.50$  Hz), 4.24–4.30 (m), 4.72 (d,  $J = 9.50$  Hz), 4.82 (s), 5.48–6.10 (m), 7.70–7.86 (m), 8.11 (d,  $J = 8.41$  Hz);  $^{13}\text{C}$  NMR (62.9 MHz,  $\text{CS}_2/\text{C}_6\text{D}_6$  2:1):  $\delta = 8.93, 10.90, 11.01, 12.06, 18.82, 19.03, 21.24, 21.41, 29.35, 30.18, 30.43, 33.64, 33.83, 39.86, 43.20, 45.09, 45.30, 45.49, 46.45, 46.79, 47.80, 49.79, 49.87, 58.23, 58.44, 62.97, 63.15, 63.35, 64.17, 69.26, 69.44, 69.57, 70.06, 70.86, 70.98, 77.18, 83.23, 124.76, 129.46, 130.40, 130.96, 135.99, 136.29, 136.50, 136.81, 137.01, 139.91, 140.28, 140.56, 141.85, 141.99, 142.17, 142.30, 142.45, 142.52, 142.57, 142.86, 142.93, 143.03, 143.37, 143.48, 144.68, 145.01, 145.53, 145.57, 145.63, 145.70, 145.77, 145.93, 145.99, 146.05, 146.23, 146.41, 146.45, 146.50, 146.54, 146.63, 146.81, 147.57, 151.90, 152.99, 153.24, 154.04, 156.27, 165.26; IR (KBr):  $\tilde{\nu} = 2924, 2861, 2780, 1720, 1271, 1099, 1019, 527$   $\text{cm}^{-1}$ ; MALDI-MS (MW = 1351):  $m/z$ : 1081 [ $M - (3\text{-cyclopentadienyl)propyltriethoxysilane} + \text{H}$ ] $^+$ ; UV/Vis (THF):  $\lambda_{\text{max}}$  ( $\epsilon$ ) = 254 (115900), 322 (34800), 430 (3500), 631 (250);  $\text{C}_{93}\text{H}_{49}\text{NO}_9\text{Si}$ : calcd C 82.59, H 3.65, N 1.04; found C 81.92, H 3.34, N 1.17.$

***N*-(3,6,9-Trioxadecyl)-2-(10-decyltrimethoxysilyl)-3,4-fulleropyrrolidine (4):** Starting materials:  $\text{C}_{60}$  (42.3 mg, 0.059 mmol), *N*-(3,6,9-trioxadecyl)-glycine (**11**) (26 mg, 0.12 mmol), 11-trimethoxysilyl undecanal (**7**) (17 mg, 0.059 mmol) dissolved in toluene (40 mL) (7 h). Eluent: toluene/ethyl acetate, 7:3,  $R_f = 0.7$ ; yield = 33.9 mg (49%) along with unreacted  $\text{C}_{60}$  (13.3 mg, 31%).  $^1\text{H}$  NMR (250 MHz,  $\text{C}_6\text{D}_6$ ):  $\delta = 0.76\text{--}0.82$  (m, 2H), 1.32–1.48 (m, 12H), 1.61–1.67 (m, 2H), 1.92–1.98 (m, 2H), 2.36–2.45 (m, 2H), 3.03–3.10 (m, 2H), 3.19 (s, 3H), 3.42–3.46 (m, 2H), 3.51 (s, 9H), 3.59–3.65 (m, 2H), 3.65–3.70 (m, 4H), 3.85–3.92 (m, 2H), 4.15 (d,  $J = 10.60$  Hz, 1H), 4.20 (t,  $J = 5.48$  Hz, 1H), 4.95 (d,  $J = 10.60$  Hz, 1H);  $^{13}\text{C}$  NMR (62.9 MHz,  $\text{C}_6\text{D}_6$ ):  $\delta = 9.93, 23.28, 27.62, 29.81, 29.94, 29.96, 30.04, 30.54, 31.62, 33.55, 50.30, 52.24, 58.74, 67.86, 71.00, 71.13, 71.18, 71.74, 72.45,$

76.68, 77.61, 135.80, 136.04, 136.62, 137.50, 140.00, 140.23, 140.50, 140.56, 142.08, 142.16, 142.38, 142.42, 142.47, 142.58, 142.65, 142.96, 143.03, 143.45, 143.56, 144.74, 144.78, 144.89, 145.05, 145.57, 145.67, 145.72, 145.91, 146.07, 146.09, 146.25, 146.31, 146.35, 146.48, 146.57, 146.65, 147.43, 147.46, 154.28, 155.49, 155.61, 157.14; IR (KBr):  $\tilde{\nu} = 2919, 2849, 1461, 1427, 1098, 1024, 802, 527$ ; MALDI-MS (MW = 1169):  $m/z$ : 1170 [ $M + \text{H}$ ] $^+$ , 720 [ $\text{C}_{60}$ ] $^+$ ; UV/Vis (THF):  $\lambda_{\text{max}}$  ( $\epsilon$ ) = 255 (90400), 318 (32600), 431 (4100), 629 (470);  $\text{C}_{82}\text{H}_{47}\text{NO}_6\text{Si}$ : calcd C 84.15, H 4.05, N 1.20; found C 82.87, H 3.60, N 0.98.

**(3-Cyclopentadienyl)propyltriethoxysilane monomer (6):** Thermal cycloreversion was achieved by heating the corresponding (3-cyclopentadienyl)propyltriethoxysilane dimer (which is commercially available as a mixture of isomers) to 195 °C at 0.5 mmHg. Under these conditions, the mixture of monomeric isomers distilled at 87–89 °C.

**11-Trimethoxysilylundecanal (7):** Hexachloroplatinic acid in cyclohexanone (10  $\mu\text{L}$  of a solution prepared by dissolving the catalyst (10 mg) in cyclohexanone (1 mL)) was added to a solution of 10-undecenal (200  $\mu\text{L}$ , 0.96 mmol) and trimethoxysilane (150  $\mu\text{L}$ , 1.18 mmol), and the reaction mixture was heated to 55 °C for 4 h. The product was purified by flash chromatography ( $\text{SiO}_2$ , eluent: petroleum ether/ethyl acetate 9:1) affording **7** (110.8 mg, 39%) as a yellowish oil.  $^1\text{H}$  NMR (250 MHz,  $\text{C}_6\text{D}_6$ ):  $\delta = 0.61\text{--}0.67$  (m, 2H), 1.26–1.40 (m, 14H), 1.59–1.65 (m, 2H), 2.41 (td,  $J = 1.8$  Hz,  $J = 7.3$  Hz, 2H), 3.56 (s, 9H), 9.76 (t,  $J = 1.8$  Hz, 1H);  $^{13}\text{C}$  NMR (62.9 MHz,  $\text{CDCl}_3$ ):  $\delta = 9.12, 22.07, 22.57, 28.15, 29.20, 29.32, 29.40, 33.10, 43.90, 50.48, 198.39$ ; IR (film):  $\tilde{\nu} = 2931, 2849, 1708, 1085, 814$   $\text{cm}^{-1}$ ; GC-MS (MW = 290):  $m/z$  (%): 91 (38), 121 (100), 177 (18), 226 (6);  $\text{C}_{14}\text{H}_{30}\text{O}_4\text{Si}$ : calcd C 57.89, H 10.41; found C 57.65, H 10.15.

**4-Formyl-2-[2-(2-hydroxyethoxy)ethoxy]ethyl benzoate:** Thionyl chloride (8 mL) was added to a suspension of 4-formylbenzoic acid (2.0 g, 13.3 mmol) in dry benzene (20 mL), and the reaction mixture was refluxed for 3 h. The excess  $\text{SOCl}_2$  and benzene were removed under reduced pressure and the resulting acid chloride was used without further purification. Triethylene glycol (10 mL, 75 mmol) and triethylamine (3.5 mL, 25 mmol) were placed in a flask (100 mL) fitted with an addition funnel, and cooled with an ice-bath. Freshly prepared 4-formylbenzoic acid chloride in dry  $\text{CH}_2\text{Cl}_2$  (20 mL) was introduced into the funnel and was added dropwise to the solution. When the addition was complete, the ice-bath was removed and the reaction mixture stirred at ambient temperature overnight. The solvent was removed in vacuo and the residue was dissolved in ethyl acetate (25 mL), and subsequently washed with a saturated solution of  $\text{Na}_2\text{HCO}_3$  and then with brine. The organic layer was dried over  $\text{Na}_2\text{SO}_4$  and was then evaporated under reduced pressure. The residue was purified by chromatography ( $\text{SiO}_2$ , eluent: toluene/ethyl acetate 1:1, then ethyl acetate) affording the desired product as a clear oil (1.2 g, 32%). IR (film):  $\tilde{\nu} = 3448, 2872, 1712, 1276, 1116, 755$   $\text{cm}^{-1}$ ;  $^1\text{H}$  NMR (250 MHz,  $\text{CDCl}_3$ ):  $\delta = 3.53$  (m, 2H), 3.63 (m, 6H), 3.78 (m, 2H), 4.44 (m, 2H), 7.86 (m, 2H), 8.12 (m, 2H), 10.01 (s, 1H);  $^{13}\text{C}$  NMR (62.9 MHz,  $\text{CDCl}_3$ ):  $\delta = 61.41, 64.29, 68.81, 70.08, 70.43, 72.34, 129.26, 130.05, 134.74, 138.95, 165.29, 191.50$ ; GC-MS (MW = 282):  $m/z$  (%): 45 (64), 77 (19), 89 (12), 105 (20), 133 (100), 177 (54);  $\text{C}_{14}\text{H}_{18}\text{O}_6$ : calcd C 59.57, H 6.43; found C 59.10, H 6.58.

**4-Formyl-2-[2-(2-acryloxyethoxy)ethoxy]ethylbenzoate (9):** 3-Bromopropionylchloride (72  $\mu\text{L}$ , 0.72 mmol) was added to a solution of 4-formyl-2-[2-(2-hydroxyethoxy)ethoxy]ethylbenzoate (200.4 mg, 0.71 mmol) and triethylamine (250  $\mu\text{L}$ , 1.79 mmol) in dry  $\text{CH}_2\text{Cl}_2$  (250  $\mu\text{L}$ , 1.79 mmol) at ambient temperature. After 24 h, the reaction mixture was diluted with  $\text{CH}_2\text{Cl}_2$  (10 mL) and washed with brine. The organic layer was dried over  $\text{Na}_2\text{SO}_4$  and evaporated under reduced pressure. The residue purified by flash chromatography ( $\text{SiO}_2$ , eluent: toluene/ethyl acetate 1:1) affording **9** (134 mg, 56%) as a yellowish oil.  $^1\text{H}$  NMR (200 MHz,  $\text{CDCl}_3$ ):  $\delta = 3.67\text{--}3.71$  (m, 4H), 3.74 (t,  $J = 4.70$  Hz), 3.85 (t,  $J = 4.70$  Hz, 2H), 4.30 (t,  $J = 4.70$  Hz, 2H), 4.51 (t,  $J = 4.70$  Hz, 2H), 5.81 (dd,  $J = 10.17$  Hz,  $J = 1.96$  Hz, 1H), 6.13 (dd,  $J = 10.17$  Hz,  $J = 17.22$  Hz, 1H), 6.41 (dd,  $J = 17.22$  Hz,  $J = 1.96$  Hz, 1H), 7.94 (d,  $J = 8.22$  Hz, 2H), 8.20 (d,  $J = 8.22$  Hz, 2H), 10.10 (s, 1H);  $^{13}\text{C}$  NMR (62.9 MHz,  $\text{CDCl}_3$ ):  $\delta = 63.50, 64.52, 69.02, 69.07, 70.54, 70.57, 128.12, 129.39, 130.18, 130.96, 134.95, 139.09, 165.41, 166.01, 191.56$ ; GC-MS (MW = 336):  $m/z$  (%): 55 (92), 77 (28), 99 (82), 133 (100), 149 (6), 177 (90), 207 (6), 264 (4);  $\text{C}_{17}\text{H}_{20}\text{O}_7$ : calcd C 60.71, H 5.99; found C 60.26, H 6.00.

**Cycloaddition of cyclopentadienyl derivative 6 to compound 9: synthesis of aldehyde 8:** A solution of alkene **9** (32 mg, 0.095 mmol) and excess freshly distilled (3-cyclopentadienyl)-propyltriethoxysilane **6** (110  $\mu\text{L}$ ) in 1,2-



dichlorobenzene (1.5 mL) was heated to 180 °C for 30 min. The solution was then loaded into the top of a SiO<sub>2</sub> column and the product was purified by flash chromatography (eluent: toluene/ethyl acetate, gradient from 9:1 to 7:3) affording **8** (53 mg, 92%) as an orange oil. The following analytical data refer to the isolated product which is a mixture of isomers. <sup>1</sup>H NMR (200 MHz, C<sub>6</sub>D<sub>6</sub>): δ = 0.55–1.05 (m), 1.23 (t, *J* = 6.84 Hz), 1.24–3.21 (m), 3.39–3.50 (m), 3.87 (q, *J* = 6.84 Hz), 4.11–4.19 (m), 4.27–4.34 (m), 5.55–5.96 (m), 7.47 (d, *J* = 8.30 Hz), 8.08 (d, *J* = 8.30 Hz), 9.56 (s); <sup>13</sup>C NMR (62.9 MHz, C<sub>6</sub>D<sub>6</sub>): δ = 10.83, 10.89, 10.96, 12.02, 18.59, 20.24, 21.29, 21.39, 29.20, 29.95, 30.35, 32.87, 33.50, 33.58, 34.65, 35.93, 42.66, 42.94, 43.28, 45.12, 45.28, 46.18, 46.28, 46.69, 46.78, 47.72, 49.54, 49.80, 50.53, 58.47, 58.68, 63.05, 63.24, 63.37, 63.45, 64.64, 69.19, 69.46, 69.48, 70.66, 70.75, 70.85, 124.74, 127.83, 128.13, 128.29, 129.37, 129.74, 130.29, 135.12, 136.53, 136.90, 137.20, 138.92, 139.56, 146.87, 152.30, 152.56, 165.34, 173.93, 174.13, 175.71, 175.89, 176.79, 190.72; C<sub>31</sub>H<sub>46</sub>O<sub>10</sub>Si: calcd C 61.36, H 7.64; found C 60.77, H 7.31.

**OL measurements:** The fluence-dependent transmission measurements were performed with 15 ns pulses from an excimer pumped dye laser (Lambda Physik FL2002) operating with Coumarin 503 and Sulforhodamin B, with measurements at 532 and 652 nm. The repetition rate of the pulses was 1 Hz and the laser beam was focused into the sample by a lens with a 200 mm focal length, which yielded an estimated beam waist in free space of ≈ 50 μm. Incident and transmitted laser pulse energies were measured with photodiodes calibrated with an absorbing calorimeter. The transmitted radiation reached the detector with an acceptance angle of about 1 × 10<sup>-2</sup> sr. For solution samples, 1 cm cuvettes were used and all the measurements for the different compounds were done in sequence, at each wavelength, without changing any optical element or alignment feature that could have affected the pulse characteristics and beam propagation properties. The possibility of sample damage was ruled out by verifying that reproducible data could be obtained from the same sample spot after cycling the laser fluence up to the maximum reported value.

## Acknowledgments

Part of this work was supported by C.N.R. through the program Materiali Innovativi (legge 95/95). We also thank the European Commission (DG XII) for financial support through Contract BRPR-CT97-0564.

- [1] R. Dagani, *Chem. Eng. News* **1996**, *74*, 24–25.
- [2] *Materials for Optical Limiting* (Eds.: R. Crane, K. Lewis, E. Van Stryland, M. Khoshnevisan), Materials Research Society, Pittsburgh, **1995**.
- [3] J. W. Perry, K. Mansour, S. R. Marder, K. J. Perry, D. Alvarez, I. Choong, *Opt. Lett.* **1994**, *19*, 625–627.
- [4] L. W. Tutt, S. W. McCahon, *Opt. Lett.* **1990**, *15*, 700–702.
- [5] S. Shi, W. Ji, S. H. Tang, J. P. Lang, X. Q. Xin, *J. Am. Chem. Soc.* **1994**, *116*, 3615–3616.
- [6] L. W. Tutt, A. Kost, *Nature* **1992**, *356*, 225–226.
- [7] H. W. Kroto, J. R. Heath, S. C. O'Brien, R. F. Curl, R. E. Smalley, *Nature* **1985**, *318*, 162–163.
- [8] W. Krätschmer, L. D. Lamb, K. Fostiropoulos, D. R. Huffman, *Nature* **1990**, *347*, 354–358.
- [9] F. Henari, J. Callaghan, H. Stiel, W. Blau, D. J. Cardin, *Chem. Phys. Lett.* **1992**, *199*, 144–148.
- [10] D. G. McLean, R. L. Sutherland, M. C. Brant, D. M. Brandelik, *Opt. Lett.* **1993**, *18*, 858–860.
- [11] C. Li, L. Zhang, R. Wang, Y. L. Song, Y. Wang, *J. Opt. Soc. Am. B* **1994**, *11*, 1356–1360.
- [12] S. Couris, E. Koudoumas, A. A. Ruth, S. Leach, *J. Phys. B* **1995**, *28*, 4537–4554.
- [13] L. Smilowitz, D. McBranch, V. Klimov, J. M. Robinson, A. Koskelo, M. Grigorova, B. Mattes, H. Wang, F. Wudl, *Opt. Lett.* **1996**, *21*, 922–924.
- [14] C. Li, J. H. Si, M. Yang, R. B. Wang, L. Zhang, *Phys. Rev. A* **1995**, *51*, 569–575.
- [15] J. W. Arbogast, A. P. Darmanian, C. S. Foote, Y. Rubin, F. N. Diederich, M. M. Alvarez, S. J. Anz, R. L. Whetten, *J. Phys. Chem.* **1991**, *95*, 11–12.
- [16] T. W. Ebbesen, K. Tanigaki, S. Kuroshima, *Chem. Phys. Lett.* **1991**, *181*, 501–504.
- [17] S. R. Mishra, H. S. Rawat, M. P. Joshi, S. C. Mehendale, *J. Phys. B* **1994**, *27*, L157–L163.
- [18] K. M. Nashold, D. P. Walter, *J. Opt. Soc. Am. B* **1995**, *12*, 1228–1237.
- [19] A. Kost, L. Tutt, M. B. Klein, T. K. Dougherty, W. E. Elias, *Opt. Lett.* **1993**, *18*, 334–336.
- [20] U. Schubert, N. Hüsing, A. Lorenz, *Chem. Mater.* **1995**, *7*, 2010–2027.
- [21] P. Judeinstein, C. Sanchez, *J. Mater. Chem.* **1996**, *6*, 511–525.
- [22] D. Avnir, *Acc. Chem. Res.* **1995**, *28*, 328–334.
- [23] D. Levy, L. Esquivias, *Adv. Mater.* **1995**, *7*, 120–129.
- [24] R. J. P. Corriu, D. Leclercq, *Angew. Chem.* **1996**, *108*, 1524–1540; *Angew. Chem. Int. Ed. Engl.* **1996**, *35*, 1420–1436.
- [25] L. L. Hench, J. West, *Chem. Rev.* **1990**, *90*, 33–72.
- [26] R. S. Ruoff, D. S. Tse, R. Malhotra, D. C. Lorents, *J. Phys. Chem.* **1993**, *97*, 3379–3383.
- [27] Y.-P. Sun, B. Ma, C. E. Bunker, B. Liu, *J. Am. Chem. Soc.* **1995**, *117*, 12705–12711.
- [28] D. Sheng, R. N. Compton, J. P. Young, G. Mamantov, *J. Am. Ceram. Soc.* **1992**, *75*, 2865–2866.
- [29] M. Maggini, G. Scorrano, M. Prato, G. Brusatin, P. Innocenzi, M. Guglielmi, A. Renier, R. Signorini, M. Meneghetti, R. Bozio, *Adv. Mater.* **1995**, *7*, 404–406.
- [30] T. W. Zerda, A. Brodka, J. Coffey, *J. Non-Cryst. Solids* **1994**, *168*, 33–41.
- [31] J. L. Anderson, Y.-Z. An, Y. Rubin, C. S. Foote, *J. Am. Chem. Soc.* **1994**, *116*, 9763–9764.
- [32] R. Signorini, M. Zerbetto, M. Meneghetti, R. Bozio, M. Maggini, C. De Faveri, M. Prato, G. Scorrano, *Chem. Commun.* **1996**, 1891–1892.
- [33] See also, A. Kraus, M. Schneider, A. Gügel, K. Müllen, *J. Mater. Chem.* **1997**, *7*, 763–765.
- [34] A. Hirsch, *The Chemistry of the Fullerenes*, Thieme, Stuttgart, **1994**.
- [35] M. Prato, *J. Mater. Chem.* **1997**, *7*, 1097–1109.
- [36] *The Chemistry of Fullerenes* (Ed.: R. Taylor), World Scientific, Singapore, **1995**.
- [37] F. Wudl, A. Hirsch, K. C. Khemani, T. Suzuki, P.-M. Allemand, A. Koch, H. Eckert, G. Srdanov, H. M. Webb, in *Fullerenes: Synthesis, Properties, and Chemistry of Large Carbon Clusters*, ACS Symposium Series Vol. 481 (Eds.: G. S. Hammond, V. J. Kuck), American Chemical Society, Washington, DC, **1992**, pp. 161–175.
- [38] F. Wudl, *Acc. Chem. Res.* **1992**, *25*, 157–161.
- [39] Y. Rubin, S. Khan, D. I. Freedberg, C. Yeretizian, *J. Am. Chem. Soc.* **1993**, *115*, 344–345.
- [40] P. Belik, A. Gügel, J. Spickermann, K. Müllen, *Angew. Chem.* **1993**, *105*, 95–97; *Angew. Chem. Int. Ed. Engl.* **1993**, *32*, 78–80.
- [41] F. Diederich, U. Jonas, V. Gramlich, A. Herrmann, H. Ringsdorf, C. Thilgen, *Helv. Chim. Acta* **1993**, *76*, 2445–2453.
- [42] B. Kräutler, M. Puchberger, *Helv. Chim. Acta* **1993**, *76*, 1626–1631.
- [43] V. M. Rotello, J. B. Howard, T. Yadav, M. M. Conn, E. Viani, L. M. Giovane, A. L. Lafleur, *Tetrahedron Lett.* **1993**, *34*, 1561–1562.
- [44] M. Tsuda, T. Ishida, T. Nogami, S. Kurono, M. Ohashi, *J. Chem. Soc. Chem. Commun.* **1993**, 1296–1298.
- [45] L. M. Giovane, J. W. Barco, T. Yadav, A. L. Lafleur, J. A. Marr, J. B. Howard, V. M. Rotello, *J. Phys. Chem.* **1993**, *97*, 8560–8561.
- [46] M. Maggini, G. Scorrano, M. Prato, *J. Am. Chem. Soc.* **1993**, *115*, 9798–9799.
- [47] M. Prato, M. Maggini, C. Giacometti, G. Scorrano, G. Sandona, G. Farnia, *Tetrahedron* **1996**, *52*, 5221–5234.
- [48] A. Bianco, M. Maggini, G. Scorrano, C. Toniolo, G. Marconi, C. Villani, M. Prato, *J. Am. Chem. Soc.* **1996**, *118*, 4072–4080.
- [49] J. L. Speier, J. A. Webster, G. H. Barnes, *J. Am. Chem. Soc.* **1957**, *79*, 974.
- [50] A. Bianco, F. Gasparrini, M. Maggini, D. Misiti, A. Polese, M. Prato, G. Scorrano, C. Toniolo, C. Villani, *J. Am. Chem. Soc.* **1997**, *119*, 7550–7554.
- [51] T. Da Ros, M. Prato, F. Novello, M. Maggini, E. Banfi, *J. Org. Chem.* **1996**, *61*, 9070–9072.
- [52] R. V. Bensasson, E. Bienvenue, J.-M. Janot, S. Leach, P. Seta, D. I. Schuster, S. R. Wilson, H. Zhao, *Chem. Phys. Lett.* **1995**, *245*, 566–570.
- [53] R. M. Williams, J. M. Zwieter, J. W. Verhoeven, *J. Am. Chem. Soc.* **1995**, *117*, 4093–4099.

- [54] Y. Nakamura, T. Minowa, S. Tobita, H. Shizuka, J. Nishimura, *J. Chem. Soc. Perkin Trans. 2* **1995**, 2351–2357.
- [55] S. Leach, M. Vervloet, A. Desprès, E. Bréheret, J. P. Hare, T. J. Dennis, H. W. Kroto, R. Taylor, D. R. M. Walton, *Chem. Phys.* **1992**, *160*, 451–466.
- [56] P. A. Miles, *Appl. Opt.* **1994**, *33*, 6965–6979.
- [57] J. W. Perry, K. Mansour, I.-Y. S. Lee, X.-L. Wu, P. V. Bedworth, C.-T. Chen, D. Ng, S. R. Marder, P. Miles, T. Wada, M. Tian, H. Sasabe, *Science* **1996**, *273*, 1533–1536.
- [58] F. Bentivegna, M. Canva, P. Georges, A. Brun, F. Chaput, L. Malier, J.-P. Boilot, *Appl. Phys. Lett.* **1993**, *62*, 1721–1723.
- [59] R. Bozio, M. Meneghetti, R. Signorini, M. Maggini, G. Scorrano, M. Prato, G. Brusatin, M. Guglielmi, in *Photoactive Organic Materials, Vol. 3/9* (Eds.: F. Kajzar, V. M. Agranovich, C. Y.-C. Lee), Kluwer, Dordrecht, **1996**, pp. 159.
- [60] M. Brunel, M. Canva, A. Brun, F. Chaput, L. Malier, J.-P. Boilot, in *Materials for Optical Limiting, Vol. 374* (Eds.: R. Crane, K. Lewis, E. V. Stryland, M. Khoshnevisan), Materials Research Society, Pittsburgh, **1995**, pp. 281.
- [61] R. Signorini, M. Zerbetto, M. Meneghetti, R. Bozio, M. Maggini, G. Scorrano, M. Prato, G. Brusatin, E. Menegazzo, M. Guglielmi in *Fullerenes and Photonics III, Vol. 2854* (Eds.: Z. H. Kafafi), SPIE, Bellingham, **1996**, pp. 130–139.
- [62] D. W. McBranch, V. Klimov, L. B. Smilowitz, M. Grigorova, J. M. Robinson, A. Koskelo, B. R. Mattes, H. Wang, F. Wudl, in *Fullerenes and Photonics III, Vol. 2854* (Eds.: Z. H. Kafafi), SPIE, Bellingham, **1996**, pp. 140–150.

Received: January 25, 1999 [F1566]